



## ***Deschampsia antarctica* population dynamics given the trends in air temperature and penguin activity**

Nataliia Miryuta<sup>1</sup>, Denys Pishniak<sup>1</sup>, Valentyna Malanchuk<sup>1</sup>, Anton Puhovkin<sup>1</sup>, Ivan Parnikoza<sup>1, 2, \*</sup>

<sup>1</sup> State Institution National Antarctic Scientific Center, Ministry of Education and Science of Ukraine, Kyiv, 01601, Ukraine

<sup>2</sup> Institute of Molecular Biology and Genetics, National Academy of Sciences of Ukraine, Kyiv, 03143, Ukraine

\* Corresponding author: ivan.parnikoza@gmail.com

**Abstract.** The main objective of the study is to describe the dynamics of the total size of *Deschampsia antarctica* population of Galindez Island, Argentine Islands, the maritime Antarctic, during 1964–2021, both in total and as eight sectoral groups of populations and eleven separate populations. The first task is to search for possible dependence of the dynamics of the total number of plants on the average monthly air temperature. Assessing the robustness of the Galindez population (G-population), sectoral groups of populations (sectoral populations), and individual populations (populations) by phase trajectories to relate them to the effects of meteorological and other variables is the next task. Methods for estimating the population size, the cover, and morphometric parameters (leaf length and flower length, respectively) of *D. antarctica* were used for the 2013/2014–2020/2021 and 2013/2014–2023/2024 seasons. Meteorological data from a long-term meteorological observations database were used. Topological analysis was used to determine population robustness. The dependence of the plants' total number dynamics in the period 1964–2021 on the average monthly air temperature in September and February was shown. The dynamics of the sectoral populations and populations were compared with meteorological variables and other factors. The general dynamic of the G-population was described by a third-degree polynomial fit. At the same time, we managed to find a connection between the G-population and air temperature only in certain critical months of seasonal development – September and February. The individual sectors of the island exhibited significantly heterogeneous plant population trends, which may be attributed to environmental heterogeneity. The topological analysis allows to expand the populations' classification under the external factors' influence in the dynamics. Changing external conditions can lead to some populations' transitioning from one robust state to another, or from an unrobust state to a robust one and *vice versa*. In particular, the penguin invasion over the past 3 years has destroyed the D4 population, whose state was described by a strange attractor over 8 seasons; the D6 population also influenced by penguins has transitioned from a stable torus state to a strange attractor state, the D10 population has transitioned from an unrobust torus state to a limit cycle state in the last three of the 11 years of research.

**Keywords:** Antarctic hairgrass, Argentine Islands, maritime Antarctic, phase trajectories, population size

### **1 Introduction**

The maritime Antarctic has become a place where significant warming has been developing in re-

cent years (Turner et al., 2005; Convey et al., 2009; Pachauri & Meyer, 2014). The response of Antarctic biota to global climate change, including the history of its adaptation and the expected future

development, has been identified by the scientific community as a priority for biological research in Antarctica (Kennicutt et al., 2014). This fact requires searching for individual objects of flora and fauna as well as identifying the parameters of these objects that respond to climate change.

One such object widely studied in response to climate change is the Antarctic hairgrass, *Deschampsia antarctica* È. Desv. (Poaceae), which proved to be a sensitive indicator of environmental changes (Fowbert & Smith, 1994; Convey, 1996a; 1996b; Gerighausen et al., 2003; Convey & Smith, 2006; Parnikoza et al., 2009). Antarctic hairgrass is one of the two vascular plant species in Antarctica, the amazing adaptability of which remains largely unexplained (Alberdi et al., 2002; Parnikoza et al., 2011; Yao et al., 2017).

The population dynamic and individual plants parameters demonstrate dependence on the conditions of region (Vera, 2011). *Deschampsia antarctica* population studies on Galindez Island, which began in the 1960s (Fowbert & Smith, 1994) and were resumed 25 years later (Parnikoza et al., 2009), demonstrated the feasibility of initiating a long-term monitoring study of the Galindez hairgrass population based on research conducted in the 1960s. A population dynamics study conducted in the 2000s found a slowdown in the population growth (Parnikoza et al., 2009). Additionally since 2007/2008 season population of *D. antarctica* has decreased influenced by rapid expansion of penguins on Galindez Island (Dykyy et al., 2018). This requires a selection of measurement parameters at different hierarchical levels. Population size is 'the tip of the iceberg' and is based on other levels of plant development and their dependence on various non-biotic and biotic factors. This parameter is the most promising for finding dependence on the climatic situation in the study region as a whole. The climatic situation should be represented by the most significant index, the dynamics of which have changed over almost 60 years and is presented by the average monthly air temperature.

At the same time, we demonstrated the possibility of using populations size indices of Antarc-

tic hairgrass and indices of adaptability for its individuals, measured annually, which we interpret as adaptability indices in previous works (Parnikoza et al., 2015). To construct and analyses phase trajectories which indicate their robustness or unrobustness, the dynamics of the following indices were used in this work: the G-population, sectoral populations', and populations' sizes, as well as the plants' morphometric indices.

The general hairgrass G-population size's dynamics on Galindez Island turned out to have an oscillatory character. Given the absence of similar studies in the region, we cannot say how widespread this trend is. However, the plant population size dynamics are known to have always been oscillating (Figs. 2, 3), as an example of the ordered structures formation. One of the main reasons for the ordering processes can be formulated as follows: space-time structures arise as a collective fluctuations manifestation due to fluctuations, their interaction, and the selection of those that have the greatest attenuation (relaxation) time. Such long-term processes are characterised by variables called 'control oscillations' (Chalyi, 1997). According to catastrophe theory, open systems that are far from equilibrium (such as the studied *D. antarctica* populations system on Galindez Island) can be under a robust 'good' or an unrobust 'bad' condition. However, this does not mean that they cannot change their state. A transition from a robust state to an unrobust state and *vice versa* is possible at changes of any parameter. Catastrophe theory proposes not to interfere with the natural events' course and to allow the system to independently go through unrobust states to a robust state (Arnold, 1992). We aim to investigate how the extremophile *D. antarctica* goes through unrobust states and directs its development to a robust state and *vice versa* under natural conditions.

The tasks of this research were to study the G-population dynamics on Galindez Island and to conduct a dynamic study of the G-population plant size depending on average monthly air temperature for the time interval 1963/1964–2020/2021 and the robustness of G-population, sectoral pop-

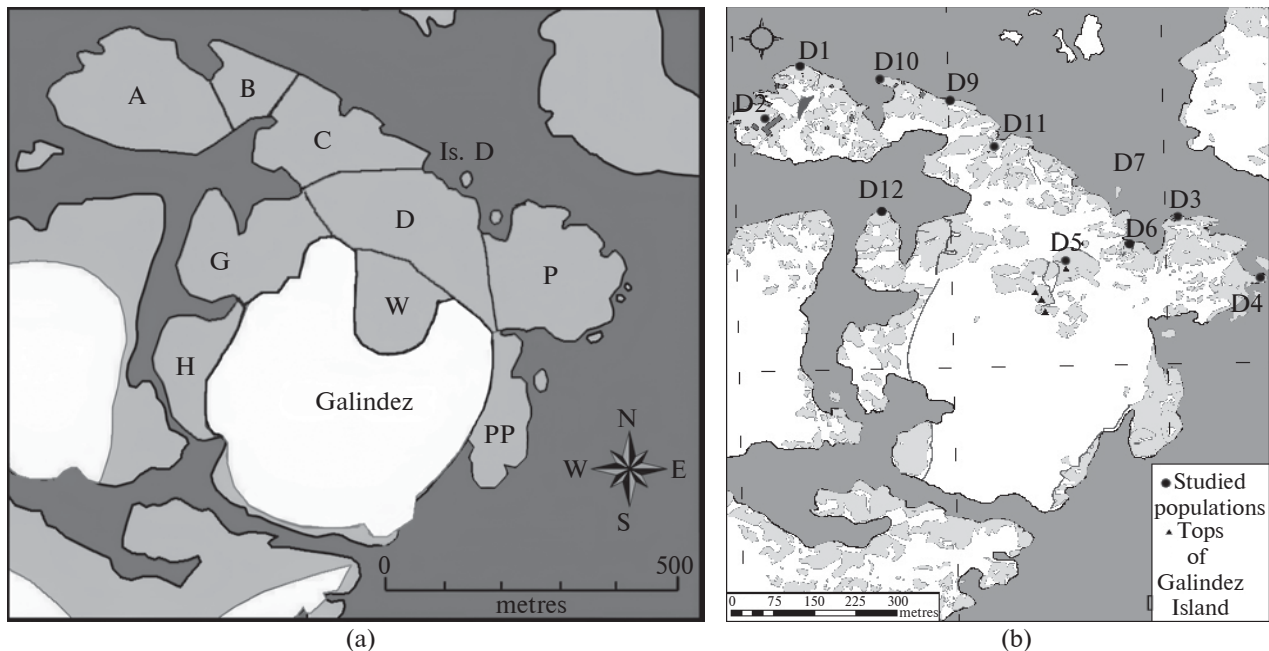


**Figure 1.** (a) – Map of the *Deschampsia antarctica* G-population sectors locations on Galindez Island: A – Marina Point, P – Penguin Point, H – Carolina Point, D – Roztochchia Ridge, Is. D – Krapla Rock, B – Shyia Ridge, C – Karpaty Ridge, G – Stella Point, PP – Pigeon Point, W – Woozle Hill. (b) – Map of the researched *D. antarctica* populations' locations on the G-population sectors of Galindez Island: D1, D2 – Marina Point (A), D3, D4 – Penguin Point (P), D5 – Woozle Hill (W), D6 – Roztochchia Ridge (D), D7 – Krapla Rock (Is. D), D9, D10 – Shyia Ridge (B), D11 – Karpaty Ridge (C), D12 – Stella Point (G)

ulations and populations by phase trajectories for the time interval 2013/2014–2020/2024 to relate them to the effect of environment variables on plants.

## 2 Materials and methods

Population studies of *Deschampsia antarctica*, which began in the 1960s (Fowbert & Smith, 1994), were resumed 25 years later (Parnikoza et al., 2009). Then, a long-term monitoring study of the G-population, sectoral populations, and individual populations was initiated on the basis of the one established in the 1960s. The plants were counted at the end of the season in February. Morphometric parameters of *D. antarctica* plants were measured from 2013/2014 to 2023/2024 as part of a monitoring study.

We will operate with the following concepts: the Galindez Island – G-population, encompass-

ing all hairgrass localities on the island; sectors of the G-population (further for convenience – sectoral populations) for parts located in different island sectors; and populations for individual populations of hairgrass distributed within some sector (G-population's sectors). The sectors on the basis of which the G-population's fragments were selected are presented in Figure 1a in accordance with (Parnikoza et al., 2009). The individual populations' distribution included in the general G-population of Galindez Island is presented in Figure 1b, published in the paper (Parnikoza et al., 2018).

The network of research sites for the regular study of *D. antarctica* populations (Fig. 1b) was established between 2006 and 2014 on Galindez Island (Miryuta et al., 2015). The locations of the monitored populations reflect the variety of growth conditions and probably represent different mic-

**Table 1.** Studied populations of *Deschampsia antarctica*,  
Galindez Island, Argentine Islands, state for 2021/2022 season

Number	Population acronym	Site description	Sectoral population
1	D <sub>1</sub> (D1)	65.244780 S, 64.255800 W, coastal rocks at Marina Point * near the meteorological station – Meteo Point ( <i>Deschampsia antarctica</i> 0.5%, mosses 0.5–40%: <i>Sanionia georgicouncinata</i> (Müll. Hal.) Ochyra & Hedenäs**, <i>Bryum pseudotriquetrum</i> (Hedw.) G. Gaertn., B. Mey. & Scherb., <i>Pohlia nutans</i> (Hedw.) Lindb., <i>Polytrichum strictum</i> Brid., <i>Warnstorffia fontinaliopsis</i> (Müll. Hal.) Ochyra, gravel, 4 m a.s.l.)	A
2	D <sub>2</sub> (D2)	65.245642 S, 64.257253 W, Marina Point, near the main station building ( <i>D. antarctica</i> 25%, mosses 65%: <i>Pohlia nutans</i> , <i>Sanionia georgicouncinata</i> , <i>Bryum pseudotriquetrum</i> , <i>Syntrichia magellanica</i> (Mont.) R.H. Zander, gravel, 12 m a.s.l.)	A
3	D <sub>3</sub> (D3)	65.247500 S, 64.241200 W, Leopard Tower, Penguin Point (northern coast, limited guano input from the nearest penguin colony, <i>D. antarctica</i> 4–19%, <i>Prasiola crispa</i> (Lightf.) Kütz. 1%, gravel, 7 m a.s.l.)	P
4	D <sub>4</sub> (D4)	65.248600 S, 64.238230 W, Korabel Rock, Penguin Point (eastern coast, limited guano input from the nearest penguin colony, <i>D. antarctica</i> 5%, mosses <1%: <i>Bryum pseudotriquetrum</i> , <i>Syntrichia magellanica</i> , <i>Prasiola crispa</i> <1%, limpet shells and gravel, 10 m a.s.l.)	P
5	D <sub>5</sub> (D5)	65.248260 S, 64.245240 W, the Eastern Terrace of the Hovorukha Dome under the Anna Hill (Woozle Hill top) (no visible guano input, <i>D. antarctica</i> 5%, mosses 45%: <i>Sanionia georgicouncinata</i> , <i>Andreaea regularis</i> Müll. Hal., <i>Polytrichum strictum</i> , gravel, 45 m a.s.l.)	W
6	D <sub>6</sub> (D6)	65.247990 S, 64.242720 W, near the <i>Colobanthus quitensis</i> (Kunth) Bartl. population, Roztochchia Ridge ( <i>D. antarctica</i> 3%, mosses 47–57%: <i>Brachythecium austrosalebrosum</i> (Müll. Hal.) Kindb., <i>B. austroglareosum</i> (Müll. Hal.) Kindb., <i>Sanionia georgicouncinata</i> , <i>Bryum pseudotriquetrum</i> , <i>Syntrichia magellanica</i> , <i>Pohlia cruda</i> (Hedw.) Lindb., <i>Bartramia patens</i> Brid., gravel, 15 m a.s.l.)	D
7	D <sub>7</sub> (D7)	65.247017 S, 64.243167 W, on the Krapla Rock ( <i>D. antarctica</i> 1–30%, mosses <1%: <i>Brachythecium austrosalebrosum</i> , <i>Bryum pseudotriquetrum</i> , <i>Sanionia georgicouncinata</i> , <i>Syntrichia magellanica</i> , gravel, limpets, 3 m a.s.l.)	Is. D
8	D <sub>8</sub> (D9)	65.245467 S, 64.249867 W, on the rocky shore of the Shyia Ridge behind the large magnetic pavilion ( <i>D. antarctica</i> 1–10%, mosses & liverworts 9–10%: <i>Syntrichia magellanica</i> , <i>Sanionia georgicouncinata</i> , <i>Pohlia nutans</i> , <i>Schistidium antarctici</i> (Cardot) L. Savicz & Smirnova, <i>Ceratodon purpureus</i> (Hedw.) Brid., <i>Polytrichastum alpinum</i> (Hedw.) G.L. Sm., <i>Pohlia cruda</i> , <i>Andreaea regularis</i> , <i>Orthogrimmia sessitana</i> (De Not.) Ochyra & Żarnowiec, <i>Barbilophozia hatcheri</i> (A. Evans) Loeske, gravel, 14 m a.s.l.)	B
9	D <sub>9</sub> (D10)	65.245008 S, 64.253205 W, on Magnit Point of the coastal rock ( <i>D. antarctica</i> 4–24%, mosses 1%: <i>Sanionia georgicouncinata</i> , <i>Bryum pseudotriquetrum</i> , <i>Syntrichia magellanica</i> , limpet shells, 3 m a.s.l.)	B
10	D <sub>10</sub> (D11)	65.246170 S, 64.248250 W, on the Cemetery Ridge near the pavilion of Very Low Frequencies ( <i>D. antarctica</i> 4–30%, mosses 1–10%: <i>Polytrichastum alpinum</i> , <i>Pohlia nutans</i> , <i>Pohlia cruda</i> , <i>Sanionia georgicouncinata</i> , <i>Syntrichia magellanica</i> , <i>Ceratodon purpureus</i> , <i>Bucklandiella sudetica</i> (Hurw.) Bednarek-Ochyra & Ochyra, <i>Bryum pseudotriquetrum</i> , <i>Andreaea regularis</i> , limpets, gravel, 17 m a.s.l.)	C
11	D <sub>11</sub> (D12)	65.247450 S, 64.252740 W, on the Gull Tower slopes on Stella Point ( <i>D. antarctica</i> 1–40%, mosses 4–10%: <i>Sanionia georgicouncinata</i> , <i>Pohlia nutans</i> , <i>Pohlia cruda</i> , <i>Polytrichum strictum</i> , <i>Bucklandiella sudetica</i> , <i>Syntrichia magellanica</i> , <i>Andreaea regularis</i> , <i>Orthogrimmia sessitana</i> , <i>Ceratodon purpureus</i> , <i>Hymenoloma crispulum</i> (Hedw.) Ochyra, gravel and limpet shells, 10 m a.s.l.)	G

\* The local toponyms are provided according to Yevchun et al. (2021). \*\* The species are provided according to Ochyra et al. (2008). The voucher bryophyte collections cited in this account are stored in the bryophyte section of the herbarium in the W. Szafer Institute of Botany, Polish Academy of Sciences, in Kraków (KRAM).

roclimatic conditions of the plant's growth on the island.

The populations' and sectoral populations' coordinates and habitat descriptions are presented in Table 1.

### **Biological methods in population research**

The first part of the study used data for the G-population on Galindez Island in 1964 and 1990 (Parnikoza et al., 2009). We also used our total estimates for the island in 2006–2021. The interval between size populations determining and plant sampling in the period 2006/2007–2020/2021 was 1–3 years.

Population size is an index that is slowly changing. In addition, it does not consider the individual plants' characteristics. We have studied biometrics (leaf length, flower length) during the past eleven years (2013/2014–2023/2024) as adaptability indices for eleven populations by the methods set described in detail in (Miryuta et al., 2015; 2019; Parnikoza et al., 2015).

### **Meteorological methods in the study of plant populations**

To find the relationship between the dynamics of the total number of plants on Galindez Island and the air temperature dynamics, we used the meteorological observations at the Faraday/Akademik Vernadsky base weather station (65.244780 S, 64.255800 W) for the years 1964–2021.

### **Statistical methods**

In the first part of the study dynamics, the G-population size and sectoral population sizes were described by third-degree polynomials selected by the least square's method (Pollard, 2009) with the program CurveExpert1.3. Average monthly air temperature data dynamics were used with a 5-year interval during the period (1964–2013) and with a 1–3-year interval for the period (2014–2021). Average monthly air temperature data dy-

namics were smoothed by linear filtration (averaging over two points). To find the correlation between the *D. antarctica*'s G-population size dynamics and the average monthly air temperature dynamics, a regression technique was used for each month of the year (Pollard, 2009; Corder & Foreman, 2014).

In the second part of the study we constructed phase trajectories in the coordinates ( $S(t)$ ,  $dS(t)/dt$ ) where  $S(t)$  was population size,  $dS(t)/dt$  was rate of change in population size. We determined the rate of change in population sizes by the finite-difference method (Pollard, 2009; Corder & Foreman, 2014). The analysis of steady state robustness is closely related to the order parameter and the principle of subordination. Until recently, such an analysis was performed for dynamic equations of a certain kind. However, this is not always sufficient given a large dataset, so the term “attractor” has been used to describe complex experimental systems (Klevecz et al., 2008). We have used theoretical concepts such as ‘attractor’ and ‘phase trajectory’ to study the experimental system, similarly to researchers of different organisms, species, and populations (Eigen & Schuster, 1979; Pechurkin et al., 1990; Chalyi, 1997; Klevecz et al., 2008; Miryuta & Kunakh, 2011).

For the phase trajectory analysis, examples of phase trajectories in coordinates ( $S$ ,  $dS/dt$ ) for different equation systems of De Boer (2025) were used, where  $S$  represents population size and  $t$  represents time.

For the topological analysis of the phase trajectories in coordinates ( $x(t)$  was population size dynamics ( $S$ ),  $y(t)$  was dynamics of average leaf length ( $dl$ ),  $z(t)$  was dynamics of average flower length ( $dk$ )), we used the method of eigenvalues (Lyapunov indices). To do this, we selected exponential curves using the CurveExpert1.3 program for the sets  $x(t) = \exp \lambda_1 t$ ,  $y(t) = \exp \lambda_2 t$ ,  $z(t) = \exp \lambda_3 t$  and determined the fit reliability. If the data were not described by the exponent, the eigenvalue  $\lambda = 0$ ; if the data were reliably described by the exponential curve, two variants ( $\lambda < 0$  and  $\lambda > 0$ ) were possible. The attractor type

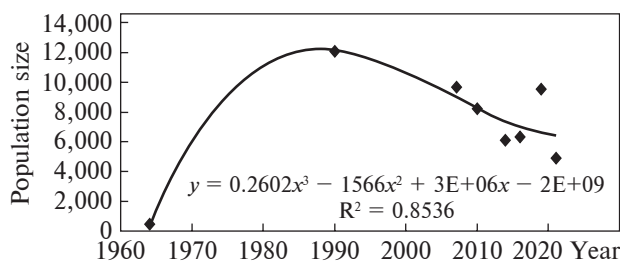


**Figure 2.** Dynamics of *Deschampsia antarctica* G-population size in Galindez Island over five decades. The set of points is adequately described by a third-degree polynomial fit (for  $R^2 = 0.8536$ ,  $N = 8$   $F_{1,6} = 34.986$ , for  $\alpha = 0.05$ , the limit value is  $F_{1,6} = 5.99$ )

was determined by a set of eigenvalues  $\lambda$  according to the classification in the works (Eigen & Schuster, 1979; Chalyi, 1997).

### 3 Results and discussion

Summary results of the G-population size in long-term studies over the decades is shown in Figure 2.

The most interesting finding of the current study is that the strong population growth trends of *Deschampsia antarctica* observed in 1990 (Fowbert & Smith, 1994) have not extend to this 2007–2021 study. Rather the *D. antarctica* plant number present on Galindez Island has generally stabilized, with values obtained in individual sectors of the island showing fluctuations in the range of 6000–8000 individuals compared to the 1990 study (12000 individuals) and these changes are small compared to the 25-fold increase between the mid-1960s and 1990 reported by Fowbert & Smith (1994). Also, as reported by the authors (Parnikoza et al., 2009), no new

*D. antarctica* plants colonies were found on the studied Galindez Island.

The maximum G-population size values correspond to a warming period. Thus, population size has decreased in the cooler period (Fig. 2, Appendix Fig. A1). The literature suggests that since about 1990 there has been both relatively lower interannual variability and little change in mean annual temperature, and it should be noted that time series analysis of both annual and seasonal mean temperatures from 1990 to 2007/2008 is non-significant (all  $P < 0.05$ ) (Parnikoza et al., 2009). It should be noted that we used the average monthly air temperatures dynamics through this studied period 1964–2021 (Appendix Fig. A1).

The research development on Galindez Island was gradual: in the early stages of the study, we had access to data on plant numbers and air temperature, so we analysed them for a whole series of studies. To confirm this thesis, the *D. antarctica* G-population size dynamics were compared with the time series of average monthly air temperatures through the years in Galindez Island using regression (Pollard, 2009). We compared the smoothed curves of the G-population size and air temperatures for each month and found significant correlations for two months (September and February) (Table 2), and the absence of such correlations in the remaining months.

The results in Table 2 indicate the presence of correlation in February and September (above the limit of the F-distribution 5% value). This fact means that the most significant factor for the G-population size is the average monthly air temperature in September and February. That is, the G-population size is the most affected by the winter air temperature (September), which means that an increase in the winter air temperature leads to an increase in the G-population size. In addition, the air temperature's influence in February (summer period) on *D. antarctica* plants G-populations' size on Galindez Island in 1964–2021 was statistically significant (Table 2). February in the maritime Antarctic is the main month

**Table 2.** *Deschampsia antarctica* G-population size dependence on average monthly air temperature in Galindez Island (correlation coefficients R)

Month	$n$	$R^2$	$F_{1, n-2}$	$F_{1, n-2}$ ( $\alpha = 0.05$ )	R
September	22	0.2841	7.940	4.35	<b>0.533</b>
January	23	0.1551	3.864	4.32	0.393
February	23	0.1809	4.641	4.32	<b>0.425</b>

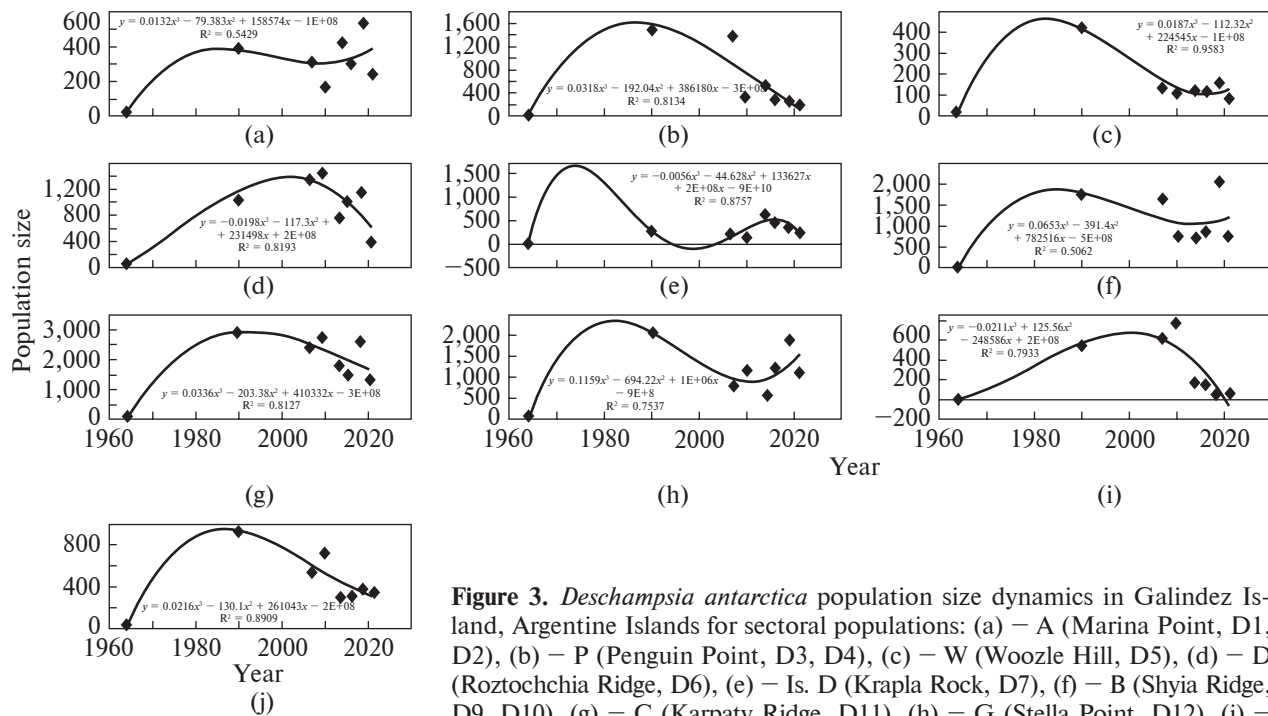


**Figure 3.** *Deschampsia antarctica* population size dynamics in Galindez Island, Argentine Islands for sectoral populations: (a) – A (Marina Point, D1, D2), (b) – P (Penguin Point, D3, D4), (c) – W (Woozle Hill, D5), (d) – D (Roztochchia Ridge, D6), (e) – Is. D (Krapla Rock, D7), (f) – B (Shyia Ridge, D9, D10), (g) – C (Karpaty Ridge, D11), (h) – G (Stella Point, D12), (i) – PP (Pigeon Point), (j) – H (Carolina Point). The set of points is adequately described by a third-degree polynomial fit, except for Is. D (Krapla Rock), which is described by a fourth-degree polynomial fit. For the smallest  $R^2 = 0.5062$ ,  $N = 8$ ,  $F_{1,6} = 6.150$ , for  $\alpha = 0.05$  the limit value is  $F_{1,6} = 5.99$

during which vegetation develops, the hairgrass inflorescences open, and the seeds ripen. The seeds form and plants accumulate substances for recovery.

The maximum G-population size corresponds to the period with more favourable conditions (higher air temperature) in February, which is changed by a G-population size decrease with a decrease in temperature this month (Appendix Fig. A1). A comparison of air temperature and G-population size sets showed a correlation in February (Table 2); however, such a dependence was not observed in December, January, and March. Air temperature in February affected the G-population size because this index indicates how favourable were the atmospheric conditions for plants during the transition to the cold season. We suppose that the air temperature in September (not February) of the previous year influenced the plant population size in February of the following year.

However, the *D. antarctica* G-population consists of sectoral populations that exist under dif-

ferent conditions. Therefore, we investigated and analysed all sectorial populations of Galindez Island, presented in Figure 3.

The sectoral population's dynamics in most cases coincided with the behaviour of the general G-population, but had its own specifics. Sectorial populations have been classified into three groups shown in Figure 3: the first – A (contains populations D1 and D2), B (contains populations D9, D10), G (contains D12), Is. D (contains D7), W (contains D5) (Fig. 3a, b, c, e, g), the second – C (contains D11), H (does not contain populations), P (contains D3, D4) (Fig. 3f, h, j), and the third – D (contains D6), PP (does not contain studied populations) (Fig. 3d, i).

For the first group, the probable first maximum is before the point determined in 1990 and passes beyond the minimum near the point determined in 2010. Furthermore, there is an increase in population size, especially noticeable in the A (populations D1, D2), B (D9, D10), and Is. D (D7) sec-

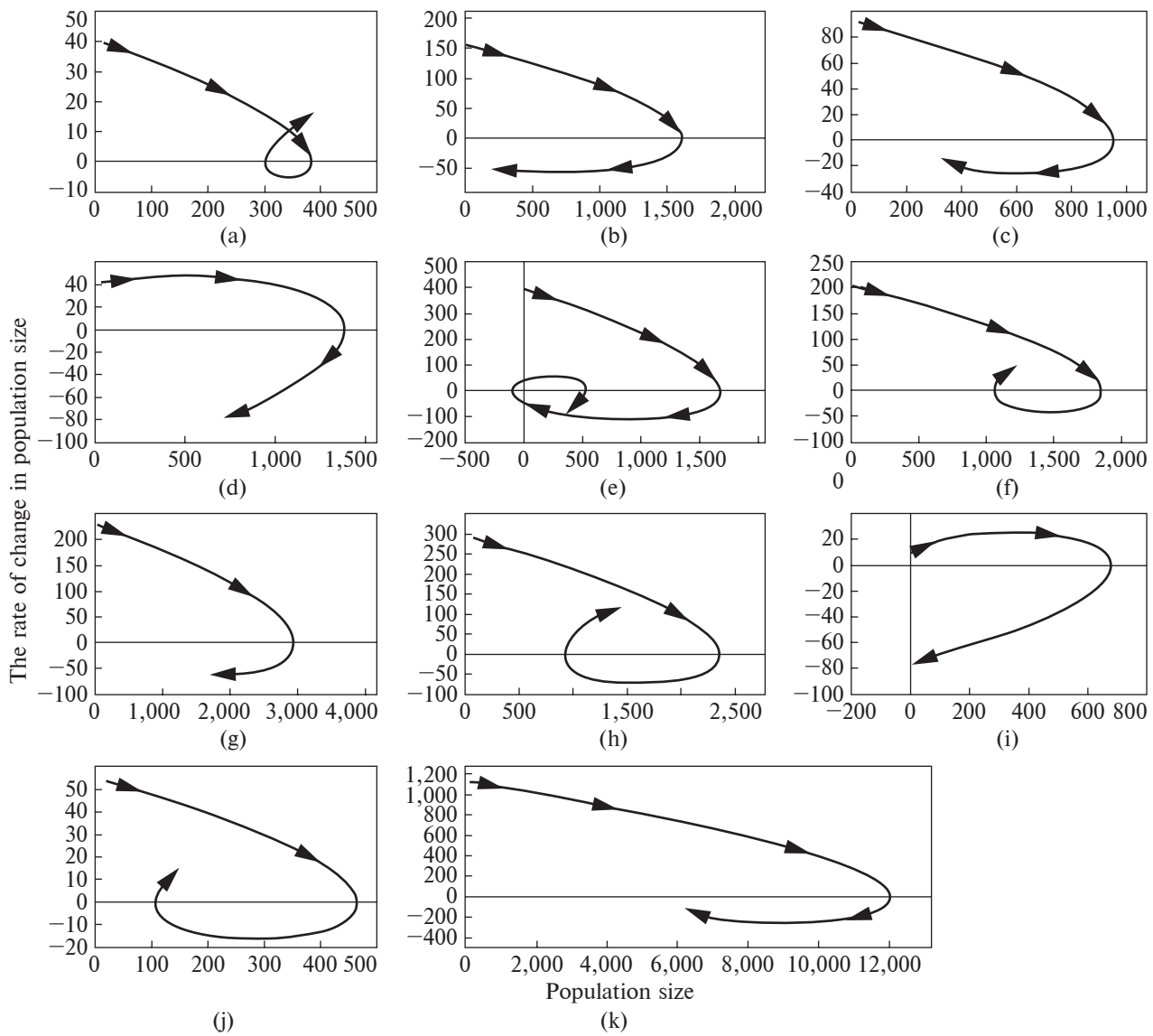


**Figure 4.** Phase trajectories (the rate of change in the population size depending on the population's size) of *Deschampsia antarctica* sectoral populations and G-population for over five decades in Galindez Island: (a) – A (Marina Point, D1, D2), (b) – P (Penguin Point, D3, D4), (c) – H (Carolina Point, D5), (d) – D (Roztochchia Ridge, D6), (e) – Is. D (Krapla Rock, D7), (f) – B (Shyia Ridge, D9, D10), (g) – C (Karpaty Ridge, D11), (h) – G (Stella Point, D12), (i) – PP (Pigeon Point), (j) – W (Woozle Hill), (k) – G-population on Galindez Island

tors. Sectoral populations of the second group are characterised by the fact that the probable first maximum occurs before the point determined in 1990 and then declines to a minimum. Such dynamics are characteristic of the G-population sectors C (D11), H (D5), and P (D3, D4). The third

group is characterised by the fact that the probable first maximum occurs after the point determined in 1990 and then decreases to a minimum. Such dynamics are characteristic of D (D6) and PP (does not contain regular studied individual populations).

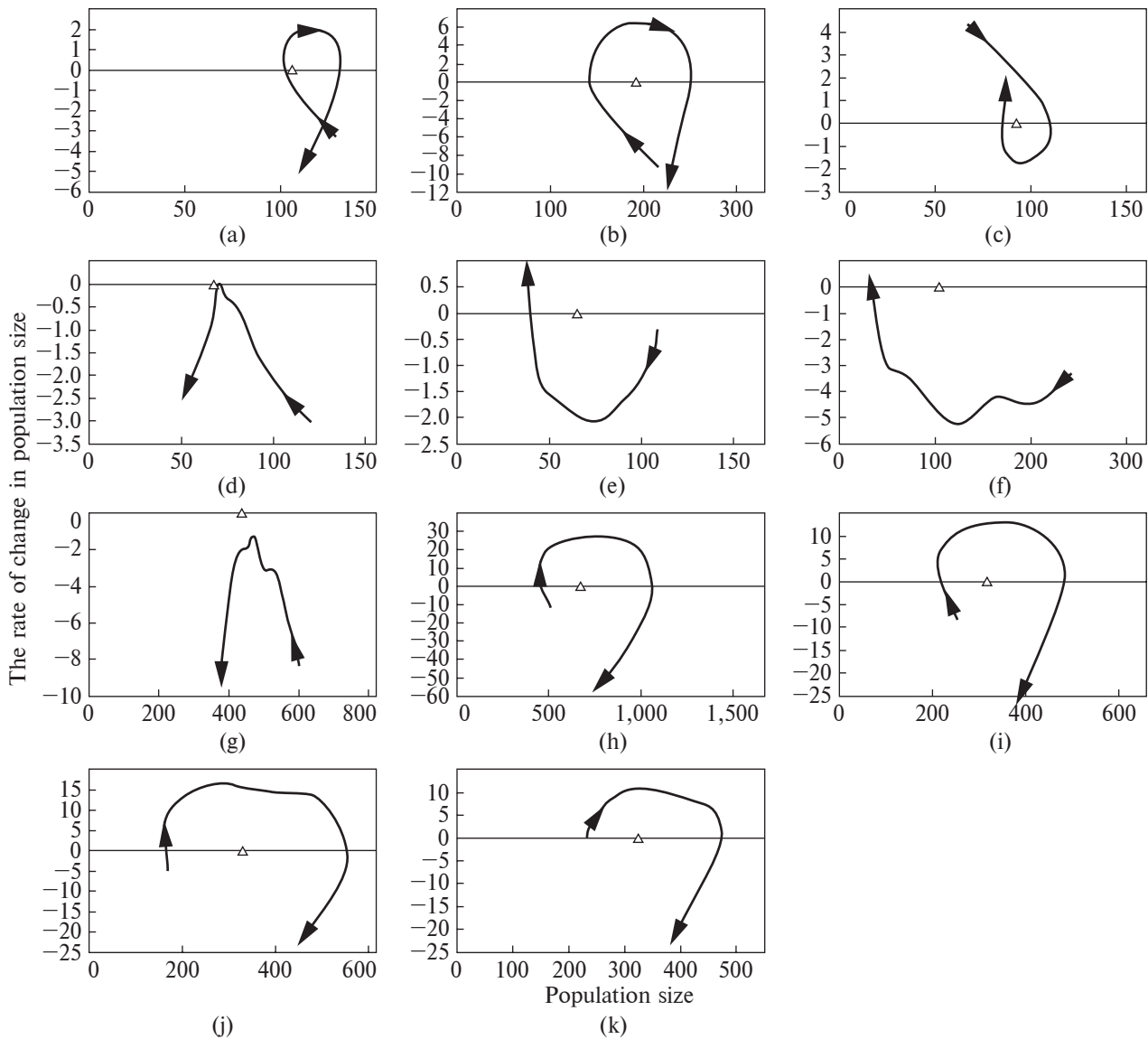


**Figure 5.** Phase trajectories of *Deschampsia antarctica* populations: (a) – D1, (b) – D2, (c) – D3, (d) – D4, (e) – D5, (f) – D6, (g) – D7, (h) – D9, (i) – D10, (j) – D11, (k) – D12 in 2010/2011–2020/2021, which at this interval (hierarchical level) are described by curves with different initial conditions than the curves in the interval 1963/1964–2020/2021. Special points are noted by triangles

Before proceeding to conclusions about the meteorological variables' impact on the plant populations, the G-population's development nature in time interval 1963/1964–2020/2021, sectoral populations in 1963/1964–2020/2021, populations in 2013/2014–2020/2021 and in 2013/2014–2023/2024 by their sizes was analysed.

The phase trajectories in coordinates  $(S, dS/dt)$  for the growth curves  $S(t)$  shown in Figure 3 were constructed by common axis extraction in the same way as was used for different species by other populations researchers (Pechurkin et al., 1990; Chalyi, 1997; Klevecz et al., 2008; Miryuta & Kunakh, 2011) and presented in Figures 4 and 5.

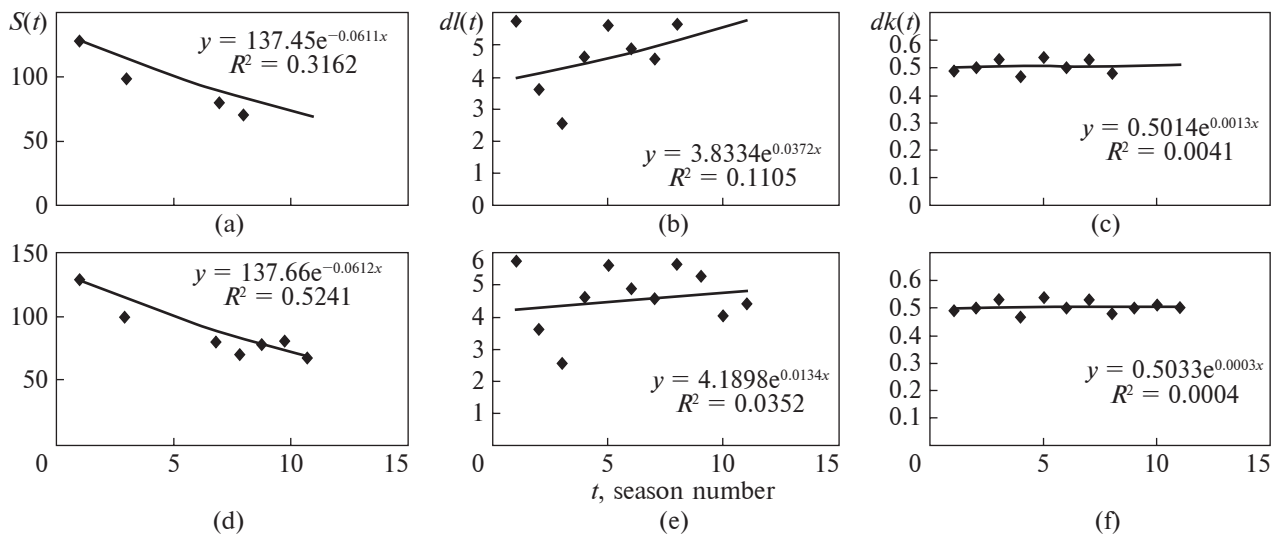


**Figure 6.** Dynamics of the plants number in D1 population (a, d), average leaf length (b, e) and average flower length (c, f) for the time intervals (season) 2013/2014–2020/2021 (a, b, c) and 2013/2014–2023/2024 (d, e, f), respectively. D1 plant population dynamics approximations by the exponential curve using the regressive technique by three indices for the intervals 1–8 (a, b, c) seasons and 1–11 (d, e, f) seasons have shown that the squares of the corresponding correlation coefficients  $R^2$  were 0.3162, 0.1105, 0.0041 (a, b, c) and 0.5241, 0.0352, 0.0004 (d, e, f), respectively. The test values for them were:  $F_{1,3} = 1.386$  (a),  $F_{1,6} = 0.744$  (b),  $F_{1,6} = 0.024$  (c) and  $F_{1,6} = 6.606$  (d),  $F_{1,9} = 0.321$  (e),  $F_{1,9} = 0$  (f), which exceed the upper 5% limit of the F-distribution value for  $N = 8$  ( $F_{1,6} = 5.99$ ) only in the case of the plants' number dynamics for 2013/2014–2023/2024 (d). This means that the eigenvalue that is not equal to zero is  $\lambda_1 < 0$  for the second period. The remaining eigenvalues are  $\lambda = 0$  for both studied periods

Figures 4 and 5 present the phase trajectories for sectoral populations (1963/1964–2020/2021) and populations (2013/2014–2020/2021), respectively.

The G-population phase trajectory in the coordinates ( $S(t)$ ,  $dS(t)/dt$ ) for the growth curve  $S(t)$  shown in Figure 2 was constructed and presented in Figure 4k. This phase trajectory is most likely to have a ‘robust focus’ attractor.

The external conditions’ influence on populations in dynamic we tried to link with population systems’ development types (phase trajectories types). In this context we based on the fact that sectoral populations and populations for research were chosen in such way: the areas where they are located have contrasting environmental microconditions.

The *D. antarctica* sectoral populations phase trajectories are shown in Figure 4; some of these probably have a ‘robust focus’ type (a, c, d, e, f, h, j) attractor. As for b, g, and i in Figure 4,

perhaps, the phase trajectory shape is determined by the presence of competitors (De Boer, 2025). Indeed, colonies of penguins could have such an impact in the case of b (P – Penguin Point, D3, D4) and i (PP – Pigeon Point) (Appendix, Table A1) and excessive snow cover in the case of g (data of our visual observations). In both cases, *D. antarctica* populations’ sizes in the sectors had a negative dependence on the number of penguin nests with eggs (Appendix, Table A2) and probably the depth of snow cover, respectively.

The phase trajectories of individual populations from 2013/2014 to 2020/2021 are shown in Figure 5. The phase trajectories in this interval are described by curves with different initial conditions than the curves in the interval 1963/1964–2020/2021.

All phase trajectories presented in Figure 5 were built on data from eight seasons. The population D1 phase trajectory (Fig. 5 a) was the change rate dependence in the plants number from plants

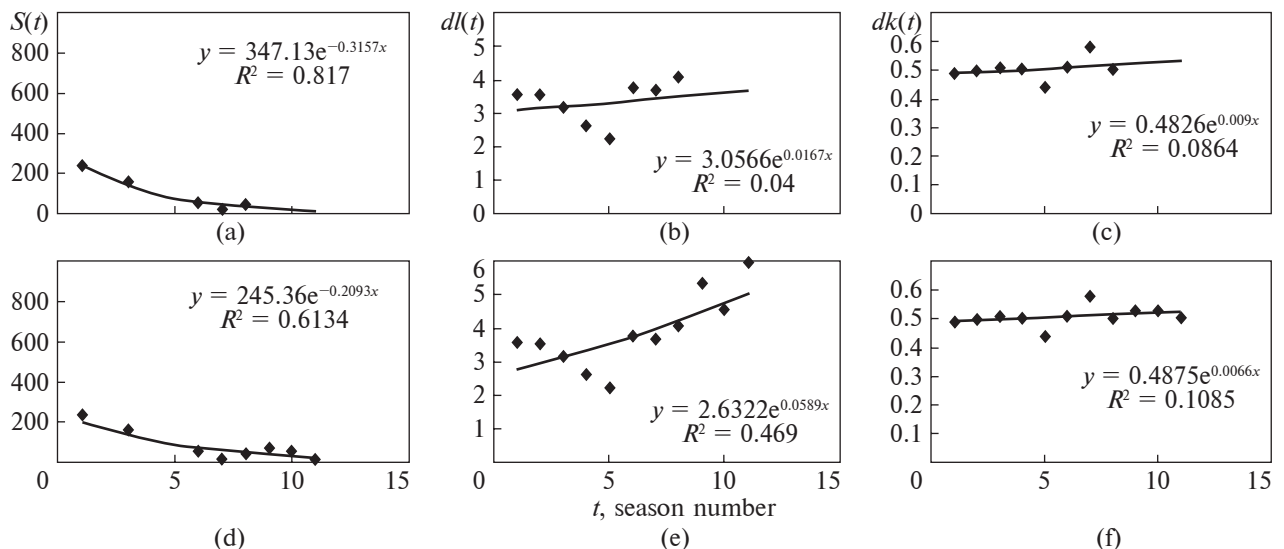


**Figure 7.** Dynamics of the plants number in D6 population (a, d), average leaf length (b, e) and average flower length (c, f) for the time intervals (seasons) 2013/2014–2020/2021 (a, b, c) and 2013/2014–2023/2024 (d, e, f), respectively. D6 plant population dynamics approximation by the exponential curve using the regressive technique by three indices for the intervals 1–8 (a, b, c) seasons and 1–11 (d, e, f) seasons has shown that the squares of the corresponding correlation coefficients  $R^2$  were 0.817, 0.04, 0.0864 (a, b, c) and 0.6134, 0.469, 0.1085 (d, e, f), respectively. The test values for them were:  $F_{1,3} = 13.992$  (a),  $F_{1,6} = 0.252$  (b),  $F_{1,6} = 0.570$  (c) and  $F_{1,6} = 9.522$  (d),  $F_{1,9} = 7.947$  (e),  $F_{1,9} = 1.098$  (f), which exceed upper 5% limit of the F-distribution value for  $N = 5$  ( $F_{1,3} = 10.13$ ),  $N = 8$  ( $F_{1,6} = 5.99$ ) only in the case of the plants number dynamics for both periods (a, d) and  $N = 11$  ( $F_{1,9} = 5.12$ ) only in the case of leaf length dynamic for the period 2013/2014–2023/2024 (e). This means that the corresponding non-zero eigenvalues are  $\lambda_1 < 0$  for both studied periods and  $\lambda_2 > 0$  for the second period. The remaining eigenvalues  $\lambda = 0$  for both studied periods (Tables 3, 4)

number. The maximum of phase trajectory speed values correspond to the plant number value  $\approx 120$ . After passing the lowest plant number values by population its size reducing the speed reduced and goes to the positive values range near a special point. Then, after reaching the maximum with terms of population size  $\approx 110$  plants, the rate began to decrease and turned into negative values.

Populations D2, D9, D10, D11, and D12 were described by phase trajectories similar to that of population D1 and were oriented clockwise. The D3 population phase trajectory differed from them because it was oriented counter clockwise. The D4 and D7 phase trajectories do not go beyond the negative values of population growth rate, i.e., at first, the rate of population decline slows down, and around a special point it starts to accelerate again. This suggests that special points of populations D4 and D7 may be saddle points. The D5 and

D6 populations' phase trajectories have special points 75 and 100 and go beyond the negative values of population growth rate, reaching the values of 40 and 25 plants populations sizes, respectively.

The *D. antarctica* plant populations on Galindez Island grow in contrasting microconditions: first of all, in differently situated parts of Galindez Island. Significant influence of penguin's invasion is observed also in case of only some populations. We estimated the eigenvalues to unambiguously characterise the behaviour of the studied dynamic systems (a transition from unstable to stable or *vice versa*) and to determine which conditions lead to the catastrophe (population collapse).

For further analysis of populations' phase trajectories, it is necessary to consider not only the plants numbers, but also other characteristics at different hierarchical levels. Such an analysis was possible for eight seasons in 11 populations.

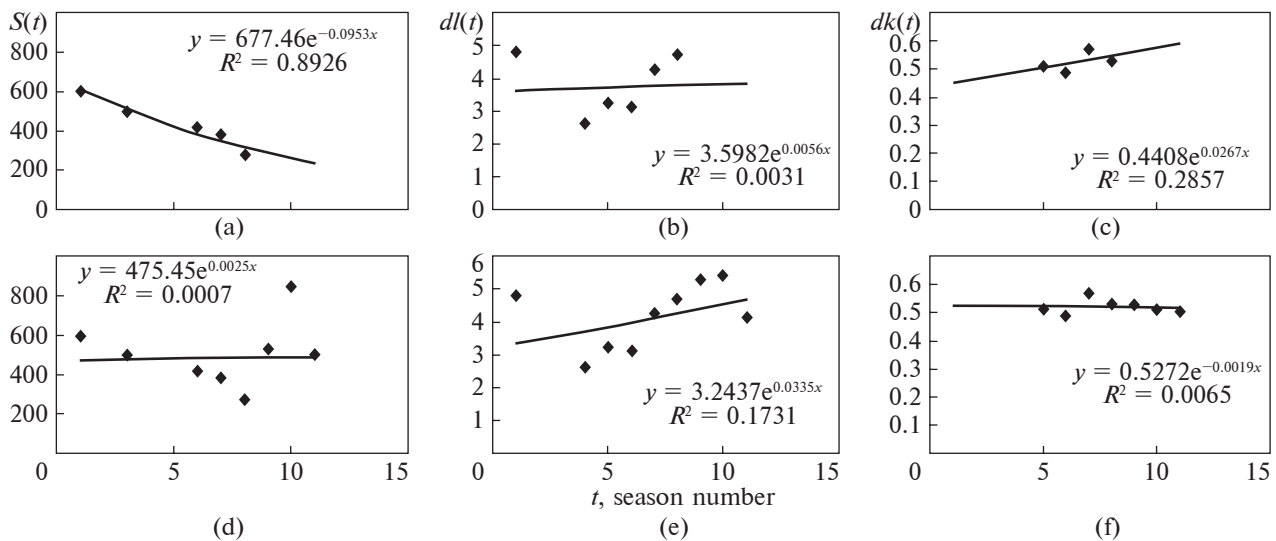


**Figure 8.** Dynamics of the plants number in D7 population (a, d), average leaf length (b, e) and average flower length (c, f) for the time intervals (season) 2013/2014 – 2020/2021 (a, b, c) and 2013/2014 – 2023/2024 (d, e, f), respectively. D7 plant population dynamics approximation by the exponential curve using the regressive technique by three indices for the intervals 1–8 (a, b, c) seasons and 1 – 11 (d, e, f) seasons has shown that the squares of the corresponding correlation coefficients  $R^2$  were 0.8926, 0.0031, 0.2857 (a, b, c) and 0.0007, 0.1731, 0.0065 (d, e, f), respectively. The test values for them were:  $F_{1,3} = 24.933$  (a),  $F_{1,6} = 0.018$  (b),  $F_{1,6} = 2.832$  (c) and  $F_{1,6} = 0.006$  (d),  $F_{1,9} = 1.881$  (e),  $F_{1,9} = 3.600$  (f), which exceed the upper 5% limit of the F-distribution value for  $N = 5$  ( $F_{1,3} = 10.13$ ) only in the case of the plants number dynamics for the period 2013/2014–2020/2021 (a). This means that the eigenvalue that is not equal to zero was  $\lambda_1 < 0$  for the first period. The remaining eigenvalues  $\lambda = 0$  for both studied periods (Tables 3, 4)

Additional data sets, in addition to the plants' number  $x(t)$  ( $S$ ), in this study were the *D. antarctica* plants' morphometric parameters: leaf length average values  $y(t)$  ( $dl$ ) and flower length  $z(t)$  ( $dk$ ) (Appendix, Tables A3, A4, A5).

To determine the attractor types, we selected exponential curves for  $x(t) = \exp(\lambda_1 t)$ ,  $y(t) = \exp(\lambda_2 t)$ ,  $z(t) = \exp(\lambda_3 t)$  using the CurveExpert1.3 program and determined the robustness of the fit. Examples are presented in Figures 6, 7, 8.

**Table 3.** Analysis of *Deschampsia antarctica* populations' robustness for 2014–2021

Population	$\lambda_1(x)$	$\lambda_2(y)$	$\lambda_3(z)$	Attractor type for three indices	Eigenvalue*
D1	0	0	0	Limit cycle	$(\lambda_1 = 0, \lambda_2 = 0, \lambda_3 = 0)$
D2	0	<0	0	Robust torus	$(\lambda_1 = 0, \lambda_2 < 0, \lambda_3 = 0)$
D3	0	0	0	Limit cycle	$(\lambda_1 = 0, \lambda_2 = 0, \lambda_3 = 0)$
D4	<0	0	>0	Chaotic (strange) attractor	$(\lambda_1 < 0, \lambda_2 = 0, \lambda_3 > 0)$
D5	<0	0	0	Robust torus	$(\lambda_1 < 0, \lambda_2 = 0, \lambda_3 = 0)$
D6	<0	0	0	Robust torus	$(\lambda_1 > 0, \lambda_2 = 0, \lambda_3 = 0)$
D7	<0	0	0	Robust torus	$(\lambda_1 < 0, \lambda_2 = 0, \lambda_3 = 0)$
D9	0	0	0	Limit cycle	$(\lambda_1 = 0, \lambda_2 = 0, \lambda_3 = 0)$
D10	0	0	>0	Unrobust torus	$(\lambda_1 = 0, \lambda_2 = 0, \lambda_3 > 0)$
D11	0	0	0	Limit cycle	$(\lambda_1 = 0, \lambda_2 = 0, \lambda_3 = 0)$
D12	0	0	>0	Unrobust torus	$(\lambda_1 = 0, \lambda_2 = 0, \lambda_3 > 0)$

\* Set of eigenvalues by which the attractor type is determined.

When the exponential curves which describe the data were not statistically reliable, the eigenvalue  $\lambda = 0$  when the exponential curve which describe the data were statistically reliably two options are possible:  $\lambda < 0$  and  $\lambda > 0$ . The type of attractor was determined for each population according to the classification provided in Eigen & Schuster (1979) and Chalyi (1997). The results for 1–8 seasons are given in Table 3.

The case when  $\lambda$  are real or complex conjugate numbers was considered. In Lyapunov indices terms, attractor types for the three indices (Table 3) were:

1. A robust focus when all  $\lambda < 0$  is the attractor. When  $\operatorname{Re} \lambda \rightarrow 0$  roots approach the imaginary axis. As a result, the initial robust focus evolves into a limit cycle, because periodic oscillations in time arise in the system (Chalyi, 1997). We can observe such oscillations in some populations (D1, D3, D9, and D11), which are given in Tables A3, A4, A5 (Appendix). As a result of these fluctuations, the system transited into a limit cycle when all  $\operatorname{Re} \lambda = 0$ ;

2. A limit cycle when all  $\operatorname{Re} \lambda = 0$  or all  $\lambda < 0$  is the attractor (special point) of the system in which undamped oscillations occur. This attractor belongs to non-coarse systems, where trajectories undergo significant changes with small variations (fluctuations) of parameters (Chalyi, 1997). D1, D3, D9, and D11 populations were in a state of a limit cycle;

3. A robust torus is an attractor if two  $\lambda = 0$ , one  $\lambda < 0$  (Chalyi, 1997). D2, D5, D6, D7 populations were in a robust torus state;

4. A chaotic (strange) attractor is formed when  $\lambda_1 > 0, \lambda_2 = 0, \lambda_3 < 0$ , has at least two special points, and the adjacent trajectories diverge under slight changes in the initial conditions (Chalyi, 1997). The D4 population was in a state of a strange attractor;

5. An unrobust torus is a phase portrait of the system, when  $\lambda_1 = 0, \lambda_2 = 0, \lambda_3 > 0$ , it is not an attractor (Chalyi, 1997). D10 and D12 populations were in an unrobust torus state.

Small changes in external parameters in the critical points region (bifurcation) can cause qualitative rearrangements (bifurcations) of the studied systems' phase portraits (Chalyi, 1997). The bifurcation results for interval 1–11 seasons are presented in Table 4.

D3, D9, and D11 populations retain their limit cycle state, while D5 retains the robust torus state, and D12 retains the unrobust torus state, as can be seen from Tables 3 and 4.

D1 population transited from the limit cycle state to the robust torus state through the transition from interval 1–8 to interval 1–11 (Tables 3, 4). We assume that this happened due to the penguins' invasion in 2022/23 and 2023/24. In this case, a bifurcation of the limit cycle into a robust torus is observed, which is part of the bifurcations:

**Table 4.** *Deschampsia antarctica* populations' robustness analysis for 2014–2024

Population	$\lambda_1(x)$	$\lambda_2(y)$	$\lambda_3(z)$	Attractors types for three indices	Eigenvalue*
D1	<0	0	0	Robust torus	$(\lambda_1 < 0, \lambda_2 = 0, \lambda_3 = 0)$
D2	<0	<0	0	Limit cycle	$(\lambda_1 < 0, \lambda_2 < 0, \lambda_3 = 0)$
D3	0	0	0	Limit cycle	$(\lambda_1 = 0, \lambda_2 = 0, \lambda_3 = 0)$
D4	—	—	—	Catastrophe	—
D5	<0	0	0	Robust torus	$(\lambda_1 < 0, \lambda_2 = 0, \lambda_3 = 0)$
D6	<0	>0	0	Chaotic (strange) attractor	$(\lambda_1 < 0, \lambda_2 > 0, \lambda_3 = 0)$
D7	0	0	0	Limit cycle	$(\lambda_1 = 0, \lambda_2 = 0, \lambda_3 = 0)$
D9	0	0	0	Limit cycle	$(\lambda_1 = 0, \lambda_2 = 0, \lambda_3 = 0)$
D10	0	0	0	Limit cycle	$(\lambda_1 = 0, \lambda_2 = 0, \lambda_3 = 0)$
D11	0	0	0	Limit cycle	$(\lambda_1 = 0, \lambda_2 = 0, \lambda_3 = 0)$
D12	0	>0	0	Unrobust torus	$(\lambda_1 = 0, \lambda_2 > 0, \lambda_3 = 0)$

\* Set of eigenvalues by which the attractor type is determined.

the old two-dimensional limit cycle → three-dimensional limit cycle, which in the open trajectories case → robust torus according to the classification given in the work (Chalyi, 1997).

The D4 population, whose state was described by a strange attractor over the 8-season period, in which the plant population number decreased because it suffered from birds and reacted by increasing the average flower size (Appendix, Table A3), was destroyed by penguins in 2022/2023.

The D6 population has transitioned from the robust torus state to the strange attractor state. This could have happened due to a change in the control parameter: the phase trajectory, which is a representation point moving along the torus, has become chaotic and moves chaotically, remaining in the strange attractor's vicinity attraction. In our case, against the background of plants number decrease in the first 8 seasons, a penguin's invasion occurred (especially in the last 3 seasons out of 11), which led to a further decrease in the plants number and a noticeable average leaf length increase (Fig. 8). That is, a bifurcation from a robust torus to a chaotic attractor has occurred.

D2 and D7 have transitioned from the robust torus state to the limit cycle state (Tables 3, 4). D7 dynamic example is presented in Figure 8. It is interesting to note that the D7 population is located on the limpet shells and may suffer from excessive humidity, whereas the D2 population, against the background of the declining G-population size, suffers due to excessive snow cover.

The D10 has transitioned from an unrobust torus state to a limit cycle state in the last three years.

## 4 Conclusions

Continuation on more early started investigation (Parnikozha et al., 2009) confirms the trend to lack of further increasing of G-population. On the contrary, the studied *Deschampsia antarctica* population rapidly decreased. The most significant impact of air temperature on the G-population size was in February (summer period) and September (winter period) for 1963/1964–2020/2021. The sec-

toral populations that were fragments of the island, were shown to have a significant heterogeneity in plant population size change trends, which may be due to environmental variation. The topological analysis allows to view the populations' classification under the influence of external factors in the dynamics. It is possible to use a spatial approach to the populations study in the season's dynamics considering their robust or unrobust state by phase trajectories to understand the development peculiarities and the cause of *D. antarctica* extremophilicity.

Changing external conditions can lead to some populations' transition from one robust state to another, or from an unrobust state to a robust one, and *vice versa*. In particular, the penguin invasion over the past 3 years has destroyed the D4 population, whose state was described by a strange attractor over 8 seasons; the D6 population has transitioned from a robust torus state to a strange attractor state, and the D10 population has transitioned from an unrobust torus state to a limit cycle state in the last three years of research.

Generally, this work has shown the possibility of applying topological analysis approach to study changes in the robust types of phase trajectories under significant changes in the environment.

**Author contributions.** N. M. – idea, statistical and topological analysis and interpretation of meteorological and biological data, drafting the manuscript. D. P. – contribution to meteorological conception and acquisition and analysis of meteorological data. V. M. – drafting and redaction of the manuscript. A. P. – preparing of field survey and laboratory measuring in season in the 2022/2023. I. P. – idea, field work, contribution to conception of meteorological factors' influences on plant populations size, manuscript processing.

**Acknowledgments.** The authors are grateful to Prof. R. Ochyra for kindly consultations in bryophyte species identification, A. Dzhulai for kindly provided data of nesting pairs quantity on Galindez Island.

**Funding.** This study was performed within the framework of the State Special-Purpose Research Program in Antarctica for 2011–2025.

**Conflict of Interest.** The authors declare no conflict of interest.

## References

Alberdi, M., Bravo, L. A., Gutiérrez, A., Gidekel, M., & Corcuera, L. J. (2002). Ecophysiology of Antarctic vascular plants. *Physiologia Plantarum*, 115(4), 479–486. <https://doi.org/10.1034/j.1399-3054.2002.1150401.x>

Arnold, V. I. (1992). *Catastrophe theory* (3rd ed). Springer. <https://doi.org/10.1007/978-3-642-58124-3>

Chalyi, O. V. (1997). *Nonequilibrium processes in physics and biology*. Naukova Dumka. (In Russian)

Convey, P. (1996a). Reproduction of Antarctic flowering plants. *Antarctic Science*, 8(2), 127–134. <https://doi.org/10.1017/S0954102096000193>

Convey, P. (1996b). The influence of environmental characteristics on life history attributes of Antarctic terrestrial biota. *Biological Reviews*, 71(2), 191–225. <https://doi.org/10.1111/j.1469-185X.1996.tb00747.x>

Convey, P., & Smith, R. I. L. (2006). Response of terrestrial Antarctic ecosystems to climate change. *Plant Ecology*, 182, 1–10. <https://doi.org/10.1007/s11258-005-9022-2>

Convey, P., Bindschadler, R., di Prisco, G., Fehrbach, F., Gutt, J., Hodgson, D. A., Mayewski, P. A., Summerhayes, C. P., & Turner, J. (2009). Antarctic climate change and the environment. *Antarctic Science*, 21(6), 541–563. <https://doi.org/10.1017/S0954102009990642>

Corder, G. W., & Foreman, D. I. (2014). *Nonparametric statistics: A step-by-step approach* (2nd ed.). Wiley.

De Boer, R. J. (2025). *Biological modeling of populations*. Utrecht University. <https://tbb.bio.uu.nl/rdb/books/bm.pdf>

Dykyy, I. V., Milinevsky, G. P., Savitsky, O. L., Lutsenko, D. G., Khoetsky, P. B., Veselsky, M. F., Smagol, V. M., Dykyy, Ye. O., Dzhulay, A. O., Tsaryk, J. V., Nazaruk, K. M., Zatushevsky, A. T., Simon, A. O., & Telipska, M. A. (2018). Features of chronology and breeding success of *Pygoscelis papua* and *P. adeliae* (*Spheniscidae*) penguins in the Wilhelm Archipelago (CCAMLR Subarea 48.1). *Ukrainian Antarctic Journal*, (17), 130–147. [https://doi.org/10.33275/1727-7485.1\(17\).2018.39](https://doi.org/10.33275/1727-7485.1(17).2018.39)

Eigen, M., & Schuster, P. (1979). *The hypercycle: a principle of natural self-organization*. Springer-Verlag, Berlin Heidelberg.

Fowbert, J. A., & Smith, R. I. L. (1994). Rapid population increases in native vascular plants in the Argentine Islands, Antarctic Peninsula. *Arctic and Alpine Research*, 26(3), 290–296. <https://doi.org/10.2307/1551941>

Gerighausen, U., Bräutigam, K., Mustafa, O., & Peter, H.-U. (2003). Expansion of vascular plants on an Antarctic island – a consequence of climate change? In A. H. L. Huiskes, W. W. C. Gieskes, J. Rozema, R. M. L. Schorno, S. M. van der Vies, & W. J. Wolff. (Eds.), *Antarctic Biology in a Global context: Proceedings of the VIIIth SCAR International Biology Symposium 27 August – 1 September 2001, Vrije Universiteit, Amsterdam, The Netherlands* (pp. 79–83). Backhuys Publishers.

Kennicutt, M. C. II, Chown, S. L., Cassano, J. J., Liggett, D., Massom, R., Peck, L. S., Rintoul, S. R., Storey, J. W. V., Vaughan, D. G., Wilson, T. J., & Sutherland, W. J. (2014). Polar research: Six priorities for Antarctic science. *Nature*, 512, 23–25. <https://doi.org/10.1038/512023a>

Klevecz, R. R., Li, C. M., Marcus, I., & Frankel, P. H. (2008). Collective behavior in gene regulation: The cell is an oscillator, the cell cycle a developmental process. *FEBS Journal*, 275(10), 2372–2384. <https://doi.org/10.1111/j.1742-4658.2008.06399.x>

Miryuta, N. Yu., & Kunakh, V. A. (2011). Dynamic of cell population systems in vitro. II. Temporal organization and robustness of *rauwolfia serpentina* benth culture tissues system at passage level. *Biotechnology*, 4(6), 18–30 (In Ukrainian)

Miryuta, N., Parnikoza, I., Shvydun, P., Myryuta, A., Poronnik, O., Kozeretska, I., & Kunakh, V. (2015). Dynamic of adaptability united latent quality indicator of *Deschampsia antarctica* population from Galindez island (Argentine Islands, maritime Antarctic) during three seasons. *Ukrainian Antarctic Journal*, (14), 143–157. <https://doi.org/10.33275/1727-7485.14.2015.183> (In Ukrainian)

Miryuta, N., Smykla, J., & Parnikoza, I. (2019). Algorithm for the United Quality Latent Index of the plant adaptability and its application field in monitoring of *Deschampsia antarctica* E. Desv. populations. *Ukrainian Antarctic Journal*, (18), 152–168. [https://doi.org/10.33275/1727-7485.1\(18\).2019.139](https://doi.org/10.33275/1727-7485.1(18).2019.139)

Ochyra, R., Smith, L. R. I., & Bednarek-Ochyra, H. (2008). *The illustrated moss flora of Antarctica*. Cambridge University Press.

Pachauri, R. K., & Meyer, L. A. (Eds.). (2014). *IPCC Climate Change 2014: Synthesis Report. Contribution of Working Groups I, II and III to the Fifth Assessment Report of the Intergovernmental Panel on Climate Change*. IPCC.

Parnikoza, I., Berezkina, A., Moiseyenko, Y., Malanchuk, V., & Kunakh, V. (2018). Complex survey of the Argentine Islands and Galindez Island (maritime Antarctic) as a research area for studying the dynamics of terrestrial vegetation. *Ukrainian Antarctic Journal*, (17), 73–101. [https://doi.org/10.33275/1727-7485.1\(17\).2018.34](https://doi.org/10.33275/1727-7485.1(17).2018.34) (In Ukrainian)

Parnikoza, I., Convey, P., Dykyy, I., Trokhymets, V., Milinevsky, G., Tyschenko, O., Inozemtseva, D., & Kozeretska, I. (2009). Current status of the Antarctic herb tundra formation in the Central Argentine Islands. *Global Change Biology*, 15(7), 1685–1693. <https://doi.org/10.1111/j.1365-2486.2009.01906.x>

Parnikoza, I., Kozeretska, I., & Kunakh, V. (2011). Vascular plants of the maritime Antarctic: Origin and adaptation. *American Journal of Plant Sciences*, 2(3), 381–395. <https://doi.org/10.4236/ajps.2011.23044>

Parnikoza, I., Miryuta, N., Ozheredova, I., Kozeretska, I., Smykla, J., Kunakh, V., & Convey, P. (2015). Comparative analysis of *Deschampsia antarctica* Desv. population adaptability in the natural environment of the Admiralty Bay region (King George Island, maritime Antarctic). *Polar Biology*, 38(9), 1401–1411. <https://doi.org/10.1007/s00300-015-1704-1>

Pechurkin, N. S., Brilkov, A. V., & Marchenkova, T. V. (1990). *Population aspects of biotechnology*. Nauka. (In Russian)

Pollard, J. H. (2009). *A handbook of numerical and statistical techniques: With examples mainly from life sciences*. <https://doi.org/10.1017/CBO9780511569692>

Turner, J., Colwell, S. R., Marshall, G. J., Lachlan-Cope, T. A., Carleton, A. M., Jones, P. D., Lagun, V., Reid, P. A., & Iagovkina, S. (2005). Antarctic climate chan-

ge during the last 50 years. *International Journal of Climatology*, 25(3), 279–294. <https://doi.org/10.1002/joc.1130>

Yao, Y., Wang, X., Li, J., Yang, J., Cao, S., Peng, F., Kurbatova, L., Peter, H.-U., Braun, C., & Li, C. (2017). A network for long-term monitoring of vegetation in the area of Fildes Peninsula, King George Island. *Advances in Polar Science*, 28(1), 23–28.

Yevchun, H., Fedchuk, A., Drohushevska, I., Pnyovska, O., Chernyshenko, M., & Parnikoza, I. (2021). The toponymy of the Argentine Islands area, the Kyiv Peninsula (West Antarctica). *Ukrainian Antarctic Journal*, (2), 127–157. <https://doi.org/10.33275/1727-7485.2.2021.683>

Vera, M. L. (2011). Colonization and demographic structure of *Deschampsia antarctica* and *Colobanthus quitensis* along an altitudinal gradient on Livingston Island, South Shetland Islands, Antarctica. *Polar Research*, 30, 7146. <https://doi.org/10.3402/polar.v30i0.7146>

Received: 18 June 2025  
Accepted: 3 November 2025

## Динаміка популяції *Deschampsia antarctica* залежно від тенденцій температури повітря та активності пінгвінів

Наталія Мірюта<sup>1</sup>, Денис Пішняк<sup>1</sup>, Валентина Маланчук<sup>1</sup>, Антон Пуговкін<sup>1</sup>, Іван Парнікова<sup>1, 2, \*</sup>

<sup>1</sup> Державна установа Національний антарктичний науковий центр, МОН України, м. Київ, 01601, Україна

<sup>2</sup> Інститут молекулярної біології та генетики, НАН України, м. Київ, 03143, Україна

\* Автор для кореспонденції: ivan.parnikoza@gmail.com

**Реферат.** Головна мета дослідження – описати динаміку загальної кількості особин *Deschampsia antarctica* на о. Галіндез (Аргентинські острови, морська Антарктика) у 1964–2021 рр. в цілому та у вигляді восьми секторальних популяцій і одинадцяти окремих популяцій. Перше завдання – дослідити можливу залежність динаміки загальної кількості рослин від середньомісячної температури повітря. Наступним завданням було оцінити стійкість популяції острова (G-популяції), секторальних популяцій та популяцій за фазовими траєкторіями, аби співвіднести їх з ефектами метеорологічних та інших змінних при виконанні наступного завдання. Методи оцінювання розміру популяції, проективного покриття та морфометричних параметрів (довжина листків та довжина квіток) *D. antarctica* були використані для сезонів 2013/2014–2020/2021 та 2013/2014–2023/2024 рр., відповідно. Джерелом метеорологічних даних була база даних довгострокових спостережень. Для визначення стійкості (робастності) популяцій використали топологічний аналіз. Було показано залежність динаміки загального числа рослин від середньої температури вересня та лютого для періоду 1964–2021 рр. Динаміки кількості секторальних популяцій та популяцій порівняли з динамікою метеорологічних змінних та інших факторів. Загальна динаміка розміру G-популяції острова була описана за допомогою полінома третього ступеня. У той же час, було виявлено зв’язок розміру G-популяції лише з температурою повітря в деякі критичні місяці сезонного розвитку (вересень, листопад). Окремі сектори, які були фрагментами острова, мали значно неоднорідні тенденції в популяціях рослин, можливо через гетерогенність умов. Топологічний аналіз дозволяє розширити класифікацію популяцій згідно з впливом зовнішніх факторів на динаміку чисельності. Зміна зовнішніх факторів може привести до переходу деяких популяцій з одного стійкого стану в інший або з нестійкого стану в стійкий чи навпаки. Зокрема розселення пінгвінів за останні три роки зруйнувало популяцію D4, стан якої протягом восьми сезонів описували моделлю дивного атрактора. Популяція D6, на яку також вплинули пінгвіни, перейшла із стабільного стану тора в стан дивного атрактора можливо внаслідок впливу пінгвінів. Популяція D10 перейшла з нестабільного стану тора в стан граничного циклу за останні три з одинадцяти років дослідження.

**Ключові слова:** Аргентинські острови, Морська Антарктика, розмір популяції, фазова траєкторія, щучник антарктичний

## APPENDIX

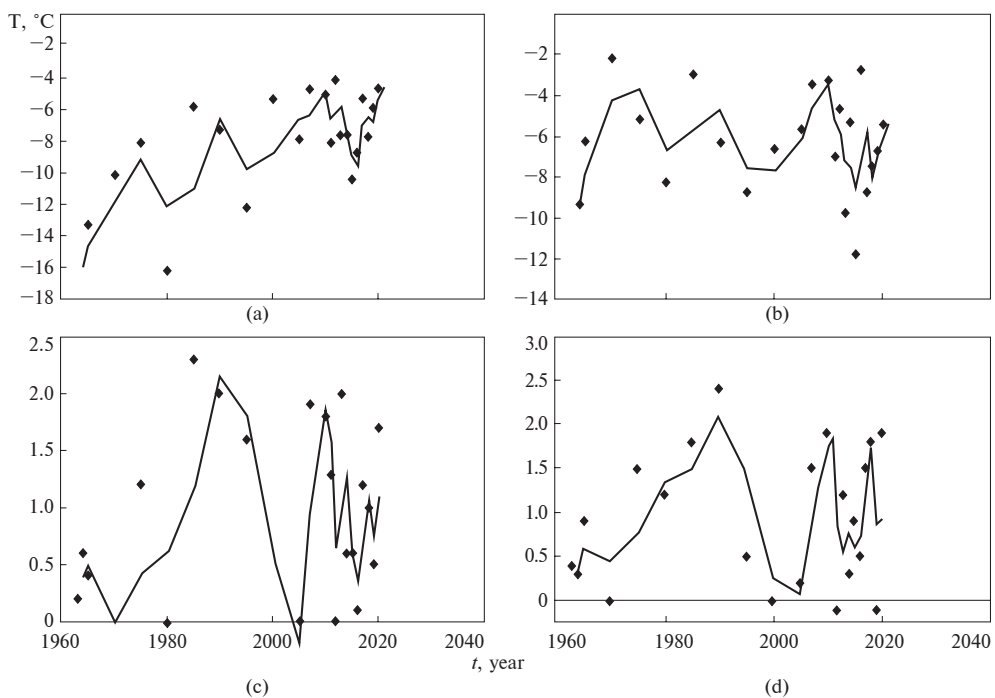


**Figure A1.** Dynamics of air temperature (a) — in August, (b) — in September, (c) — in January, (d) — in February, smoothed by linear filtration (averaging over two points) for  $n = 19$

**Table A1.** Snow cover influence on the sectoral *Deschampsia antarctica* population size (correlation coefficient R)

Sector	Month	$n$	$R^2$	$F_{1,n-2}$	$F_{1,n-2} (\alpha = 0.05)$	R
Karpaty Ridge (C)	12	12	0.4068	6.860	4.96	<b>-0.638</b>
Karpaty Ridge (C)	01	12	0.3514	5.420	4.96	<b>-0.593</b>

Note:  $n$  is the number of the studied Antarctic seasons,  $R^2$  is the square of the correlation coefficient,  $F_{1,n-2}$  is the test value,  $F_{1,n-2} (\alpha = 0.05)$  is the upper 5% F distribution limit, R is the correlation coefficient that is equivalent to the indices of the snow cover's influence on the sectoral *D. antarctica* populations' sizes.

**Table A2.** Influence of the number of penguin nests with eggs on the *Deschampsia antarctica* sectoral population size for 2009/2010–2020/2021 (correlation coefficient R)

Sector	$R^2$	$F_{1,n-2}$	R
Marina Point (A)	0.6518	18.720	<b>0.807</b>
Penguin Point (P)	0.5287	11.220	<b>-0.727</b>
Pigeon Point (PP)	0.5253	11.070	<b>-0.725</b>
Galindez Total	0.1951	2.420	0.440

Note:  $n$  is the Antarctic seasons studied number,  $R^2$  is the square of the correlation coefficient,  $F_{1,n-2}$  is the test value,  $F_{1,n-2} (\alpha = 0.05) = 4.96$  is the upper 5% F distribution limit for  $n = 12$ , R is the correlation coefficient that is equivalent to the penguin nests number with eggs influence indices on the sectoral *D. antarctica* populations' sizes.

**Table A3.** *Deschampsia antarctica* populations number during the period 2013/2014–2023/2024 seasons

Season	D1	D2	D3	D4	D5	D6	D7	D9	D10	D11	D12
2013/2014	128	216	67	117	109	240	600	500	250	170	230
2015/2016	99	124	106	80	91	161	500	547	256	242	300
2018/2019	155	330	110	66	44	57	418	1376	615	687	563
2019/2020	80	127	57	49	38	19	382	455	245	281	283
2020/2021	66	164	121	26	44	45	275	493	216	264	241
2021/2022	78	40	159	18	54	71	530	750	413	768	440
2022/2023	89	40	155	0	65	58	850	510	12	717	884
2023/2024	67	12	70	0	38	17	506	123	8	33	352

**Table A4.** Mean sample values of leaf length (cm) in *Deschampsia antarctica* populations during the period 2013/2014–2023/2024

Season	D1	D2	D3	D4	D5	D6	D7	D9	D10	D11	D12
2013/2014	5.77	5.51	5.31	3.00	3.34	3.61	4.79	5.44	4.52	4.02	4.98
2014/2015	3.63	4.44	5.43	3.14	3.62	3.57	—*	3.33	2.68	4.55	2.43
2015/2016	2.58	2.86	3.35	2.64	2.42	3.18	—	3.15	3.31	2.90	3.00
2016/2017	4.64	2.76	3.63	3.49	2.70	2.65	2.62	3.96	2.63	2.52	3.84
2017/2018	5.60	2.68	4.28	2.10	2.20	2.24	3.25	2.46	3.17	2.14	3.70
2018/2019	4.89	2.92	2.92	2.70	1.97	3.77	3.13	3.24	3.37	3.04	4.19
2019/2020	4.58	3.11	6.03	3.14	2.84	3.69	4.27	3.41	3.76	2.96	3.97
2020/2021	5.65	2.51	4.67	2.93	3.26	4.10	4.74	4.60	3.66	3.87	4.44
2021/2022	5.29	1.92	6.38	4.12	3.67	5.38	5.29	4.91	4.56	4.79	5.08
2022/2023	4.06	2.60	5.21	—**	3.80	4.60	5.41	4.54	3.95	5.16	5.17
2023/2024	4.43	1.61	4.66	—	3.44	5.97	4.15	5.44	3.42	4.37	5.40

\* Means no data. \*\* The population disappeared.

**Table A5.** Mean sample values of flower length (cm) in *Deschampsia antarctica* populations during the period 2013/2014–2023/2024

Season	D1	D2	D3	D4	D5	D6	D7	D9	D10	D11	D12
2013/2014	0.49	0.43	0.50	0.44	0.46	0.49	—*	0.49	0.40	0.48	0.47
2014/2015	0.50	0.50	0.60	0.42	0.40	0.50	—	—	—	0.46	0.50
2015/2016	0.53	0.51	0.48	0.45	0.50	0.51	—	0.49	0.47	0.49	0.49
2016/2017	0.47	0.46	0.49	0.47	0.42	0.50	—	0.44	0.46	0.40	0.47
2017/2018	0.54	0.54	0.52	0.51	0.42	0.44	0.51	0.48	0.52	0.49	0.52
2018/2019	0.50	—**	0.48	0.53	0.44	0.51	0.49	0.46	0.52	0.55	0.53
2019/2020	0.53	0.40	0.57	0.52	0.49	0.58	0.57	0.54	0.54	0.53	0.55
2020/2021	0.48	—	0.49	0.55	0.47	0.50	0.53	0.56	0.48	0.55	0.58
2021/2022	0.50	—	0.50	0.51	0.50	0.53	0.53	0.49	0.51	0.54	0.51
2022/2023	0.51	—	0.52	—***	0.49	0.53	0.51	0.51	0.49	0.50	0.51
2023/2024	0.50	—	0.51	—	0.49	0.50	0.50	0.51	0.51	0.51	0.50

\* Means no data. \*\* There were no flower stalks. \*\*\* The population disappeared.